International Journal of Renewable Energy Technology Research
Vol. 3, No. 7, July 2014, pp. 1 - 14, ISSN: 2325 - 3924 (Online)
Available online at http://ijretr.org

Research article

Design and Experimental Evaluation of the Flywheel Energy Storage System

Jun-Ho Lee[*], Byeong-Song Lee[*]

[*]Korea Railroad Research Institute

#176, Cheoldo bangmulgwan-ro, Uiwang, Gyeonggi-Do, 437-757, Korea

82+31+460+5040, jhlee77@krri.re.kr,

82-31-460-5404, bslee@krri.re.kr,

Abstract

Design and experimantal evaluation of the flywheel energy storage system(FESS) to store regenerative energy which might be generated during the braking period of the trains is presented. The proposed FESS is small scale model and has 5kW output power, high rotational speed. In general railway trains generate regenerative energy for 10-20 sec when the train brakes and also high traction energy is needed for very short moment (10 sec) when the train increases the traction force. Considering such characteristics of the railway system energy storage system for the railway should have very fast response property. Among the various energy storage systems flywheel energy storage system has the fastest response property, which means that flywheel ESS is the most suitable for the railway system.

Keywords: Magnetic Bearings, Active control, Flywheel, Railway, Energy Storage

International Journal of Renewable Energy Technology Research
Vol. 3, No. 7, July 2014, pp. 1 - 14, ISSN: 2325 - 3924 (Online)
Available online at http://ijretr.org

Introduction

Flywheel energy storage system is used to store excess electrical energy into mechanical rotational energy. The stored rotational energy is converted into electrical energy to supply that energy to the electrical machines etc. when it is needed. In order to make energy conversion between the electrical and mechanical energy or mechanical and electrical energy a power conversion device, high speed rotational flywheel to store rotational energy, rotational rotor, bearings to support the high speed rotational rotor, and housing are needed [1]-[5].

In general railway trains generate regenerative energy for 10-20 sec when the train brakes, on the other hand high traction energy is needed for very short moment (10 sec) when the train increases the traction force. Considering such characteristics of the railway system energy storage system for the railway should have very fast response property. Among the various energy storage systems flywheel energy storage system has the fastest response property, which means that flywheel ESS is the most suitable for the railway system [6].

Many researchers have invested their effort to develop flywheel ESS with focusing on the development of the high speed flywheel module rather than the system level development including an operational system for the energy conversion. The major groups for the flywheel ESS are KTSi(Kinetic Traction System Inc.), Vycon, University of Virginia, KRRI(Korea Railroad Research Institute), Piller Power Systems, etc. Among them KTSi and KRRI have tried to develop flywheel ESS which is applicable to the railway system. KTSi has tested its flywheel ESS in the Bombardier light rail test track in 2012 which is in Kingston, Canada. It has 35,000rpm operational speed, 200kW*2, and completely passive type. On the other hand KEPRI (Korea Electrical Power Research Institute) has tried to develop 100kWh, 350kW/unit super conductor flywheel ESS, however due to the high energy capacity to implement they seem to be in trouble [7].

In this paper the system configuration for the flywheel ESS including operational system for the energy conversion and the design and manufacturing of small-scale flywheel energy storage system (five-degrees-of-freedoms) supported by magnetic bearings are presented

The effectiveness of the proposed flywheel energy storage system is shown based on the high speed rotational test and also the applicability of the proposed configurations to the railway system is presented by using the energy conversion of the flywheel energy storage system that indicates the charging of the regenerative energy and discharging for the traction force based on the load test..

Materials and Method

Mathematical model

Fig. 1 presents a flywheel rotor supported by the magnetic bearings which has four-degrees-of-freedom. For the rotational rotor, left and right electromagnetic bearings support the rotor to make levitation so that the rotor can rotate without any contact with the stator. Displacement sensors are attached to very close to the electromagnetic bearings to make feedback of the displacement deviation which make it possible for the rotor to be controller actively.

Equation of motion of the rotor shown in Fig. 1 is such as:

$$M\ddot{q} + G\dot{q} = {}_{M}T_{B}u_{AMB}$$
$$y = {}_{S}T_{M}q \quad (1)$$

where

$$M=\begin{bmatrix} I_y & 0 & 0 & 0 \\ 0 & m & 0 & 0 \\ 0 & 0 & I_x & 0 \\ 0 & 0 & 0 & m \end{bmatrix}, G=\begin{bmatrix} 0 & 0 & I_z\Omega & 0 \\ 0 & 0 & 0 & 0 \\ -I_z\Omega & 0 & 0 & 0 \\ 0 & 0 & 0 & 0 \end{bmatrix},$$
$$ {}_M T_B=\begin{bmatrix} a & b & 0 & 0 \\ 1 & 1 & 0 & 0 \\ 0 & 0 & a & b \\ 0 & 0 & 1 & 1 \end{bmatrix}, {}_S T_M=\begin{bmatrix} c & 1 & 0 & 0 \\ d & 1 & 0 & 0 \\ 0 & 0 & c & 1 \\ 0 & 0 & d & 1 \end{bmatrix} \quad (2)$$

$$q=(\beta, x, -\alpha, y)^T$$
$$u_{AMB}=(f_{xA}, f_{xB}, f_{yA}, f_{yB})^T$$
$$y=(x_{sA}, x_{sB}, y_{sA}, y_{sB})^T \quad (3)$$

M is the mass matrix that is composed of mass and moment of inertia, G is the gyroscope matrix that is 0 when the rotor stops, however the amplitude becomes greater gradually as the rotational speed goes up. ${}_M T_B$ is the transformation matrix to transform the bearing coordinates to mass center coordinates, and ${}_S T_M$ is the transformation matrix to transform mass center coordinates to displacement sensor coordinates. q is the vector that expresses the position of the radial directions and the rotational angles in the mass center coordinates. u_{AMB} the force that is generated from the magnetic bearings, and y is the distance that is measured from the displacement sensor to the rotor.

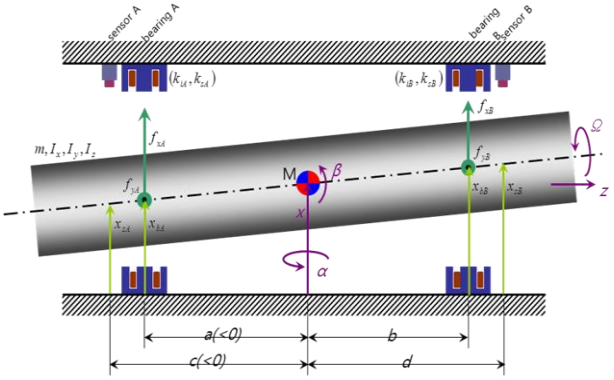

Fig. 1: Flywheel rotor which has four-degrees-of-freedom-

u_{AMB} should be linearized to design the active controller. Eqn.(4) represents the linearized model of the four-degrees-of-freedom model. In eqn. (4) K_s is the displacement stiffness that makes the system, K_i is the current stiffness, q_B is the vector that indicates the distance from the bearing location to the rotor, and i is the current vector for the bearings.

$$\begin{aligned} u_{AMB} = \begin{bmatrix} f_{xA} \\ f_{xB} \\ f_{yA} \\ f_{yB} \end{bmatrix} &= -\begin{bmatrix} k_{sA} & 0 & 0 & 0 \\ 0 & k_{sB} & 0 & 0 \\ 0 & 0 & k_{sA} & 0 \\ 0 & 0 & 0 & k_{sB} \end{bmatrix} \begin{bmatrix} x_{bA} \\ x_{bB} \\ y_{bA} \\ y_{bB} \end{bmatrix} \\ &\quad + \begin{bmatrix} k_{iA} & 0 & 0 & 0 \\ 0 & k_{iB} & 0 & 0 \\ 0 & 0 & k_{iA} & 0 \\ 0 & 0 & 0 & k_{iB} \end{bmatrix} \begin{bmatrix} i_{xA} \\ i_{xB} \\ i_{yA} \\ i_{yB} \end{bmatrix} \\ &= -K_s q_B + K_i i \end{aligned} \tag{4}$$

From the eqn. (1) and eqn. (4) the linearized equation of motion is such as:

$$M\ddot{q} + G\dot{q} = {}_M T_B(-K_s q_B + K_i i) \tag{5}$$

The vector q_B is transformed to mass center coordinates by using the transformation matrix ${}_M T_B$ which is expressed as

$$\begin{aligned} q_B = \begin{bmatrix} x_{bA} \\ x_{bB} \\ y_{bA} \\ y_{bB} \end{bmatrix} = \begin{bmatrix} a & 1 & 0 & 0 \\ b & 1 & 0 & 0 \\ 0 & 0 & a & 1 \\ 0 & 0 & b & 1 \end{bmatrix} \begin{bmatrix} \beta \\ x \\ -\alpha \\ y \end{bmatrix} &= {}_B T_M q \\ &= \left({}_M T_B \right)^T q \end{aligned} \tag{6}$$

Substituting eqn. (6) for eqn. (5) yields

$$\begin{aligned} M\ddot{q} + G\dot{q} &= -{}_M T_B K_s {}_M T_B{}^T q + {}_M T_B K_i i \\ &= -K_{sM} q + {}_M T_B K_i i \\ M\ddot{q} + G\dot{q} + K_{sM} q &= {}_M T_B K_i i \end{aligned} \tag{7}$$

where

$$K_{sM} = {}_{M}T_{B} K_{s} {}_{M}T_{B}^{T} = \begin{bmatrix} K_{sM11} & K_{sM12} & 0 & 0 \\ K_{sM12} & K_{sM22} & 0 & 0 \\ 0 & 0 & K_{sM33} & K_{sM34} \\ 0 & 0 & K_{sM43} & K_{sM44} \end{bmatrix}$$

$$K_{sM11} = k_{sA}a^2 + k_{sB}b^2,\ K_{sM33} = k_{sA}a^2 + k_{sB}b^2$$
$$K_{sM12} = k_{sA}a + k_{sB}b, \quad K_{sM34} = k_{sA}a + k_{sB}b$$
$$K_{sM21} = k_{sA}a + k_{sB}b, \quad K_{sM43} = k_{sA}a + k_{sB}b$$
$$K_{sM22} = k_{sA} + k_{sB}, \quad K_{sM44} = k_{sA} + k_{sB}$$

As seen in eqn. (7) the mathematical model of the four-degrees-of-freedom rotational machine supported by magnetic bearings is very similar to the 2nd order mechanical system. However the rotor shaft is coupled due to the gyroscopic effect and the non-colocation problem between the displacement sensors and the magnetic bearing actuators as shown in the eqn. (7).

Voltage equations for the magnetic bearing coil are expressed in eqn. (8).

$$V = Ri + L\frac{di}{dt} - K_i \frac{dq_B}{dt} \tag{8}$$

Eqn. (8) can be modified to present matrix pattern as:

$$\begin{bmatrix} v_{xA} \\ v_{xB} \\ v_{yA} \\ v_{yB} \end{bmatrix} = \begin{bmatrix} R_A & 0 & 0 & 0 \\ 0 & R_B & 0 & 0 \\ 0 & 0 & R_A & 0 \\ 0 & 0 & 0 & R_B \end{bmatrix} \begin{bmatrix} i_{xA} \\ i_{xB} \\ i_{yA} \\ i_{yB} \end{bmatrix}$$
$$+ \begin{bmatrix} L_A & 0 & 0 & 0 \\ 0 & L_B & 0 & 0 \\ 0 & 0 & L_A & 0 \\ 0 & 0 & 0 & L_B \end{bmatrix} \begin{bmatrix} \dot{i}_{xA} \\ i_{xB} \\ i_{yA} \\ i_{yB} \end{bmatrix}$$
$$- \begin{bmatrix} k_{iA} & 0 & 0 & 0 \\ 0 & k_{iB} & 0 & 0 \\ 0 & 0 & k_{iA} & 0 \\ 0 & 0 & 0 & k_{iB} \end{bmatrix} \begin{bmatrix} \dot{x}_{bA} \\ x_{bB} \\ y_{bA} \\ y_{bB} \end{bmatrix} \tag{9}$$

From eqn. (9) and by using transformation matrix ${}_{M}T_{B}$ current slew rate is derived.

$$\frac{di}{dt} = L^{-1}V - L^{-1}Ri + K_i^{-1}K_s \frac{dq_B}{dt}$$
$$= L^{-1}V - L^{-1}Ri + K_i^{-1}K_{s\,M}T_B^T \frac{dq}{dt} \quad (10)$$

The state space model for the four-degrees-of-freedom flywheel rotor can be presented by using eqn. (8) – (10).

$$\begin{bmatrix} \dot{q} \\ \dot{q} \\ i \end{bmatrix} = \begin{bmatrix} 0 & I & 0 \\ -M^{-1}K_{sM} & -M^{-1}G & -M^{-1}{}_M T_B K_i \\ 0 & K_i^{-1}K_{s\,M}T_B^T & -L^{-1}R \end{bmatrix} \begin{bmatrix} q \\ \dot{q} \\ i \end{bmatrix} + \begin{bmatrix} 0 \\ 0 \\ L^{-1}V \end{bmatrix} \quad (11)$$

FESS configuration

Fig. 2 shows the overall system configuration that consists of flywheel system, vacuum pump, and levitation controller. The flywheel system has the flywheel rotor and the housing that rotational motor stator, upper, lower, and thrust magnetic bearings are to be installed in it. The vacuum pump is connected with the housing to make vacuum the inside of the hosing, which increases the efficiency of the power conversion. The levitation controller levitates the rotor and controls the vibration of the rotor during the high speed rotation.

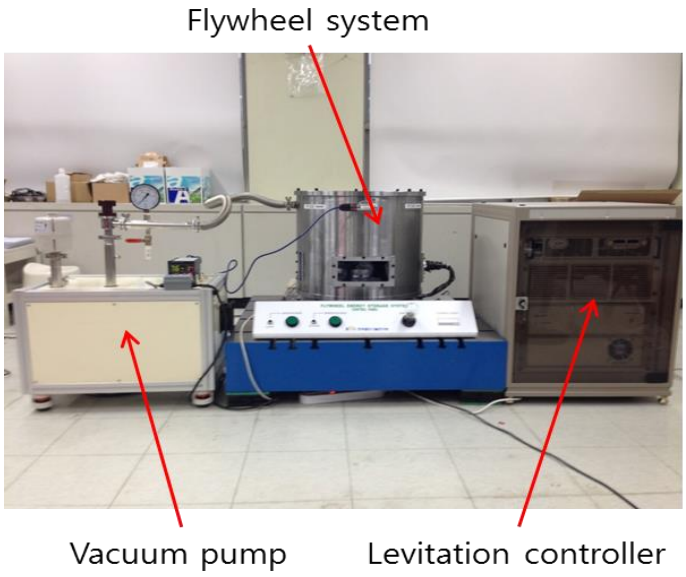

Fig. 2: FESS (Flywheel Energy Storage System) configuration

International Journal of Renewable Energy Technology Research
Vol. 3, No. 7, July 2014, pp. 1 - 14, ISSN: 2325 - 3924 (Online)
Available online at http://ijretr.org

Design of rotational rotor

One of the important issues in the design of the flywheel energy storage system is to design and to analysis of the rotational rotor. Fig. 3 shows the shape of the rotational rotor.

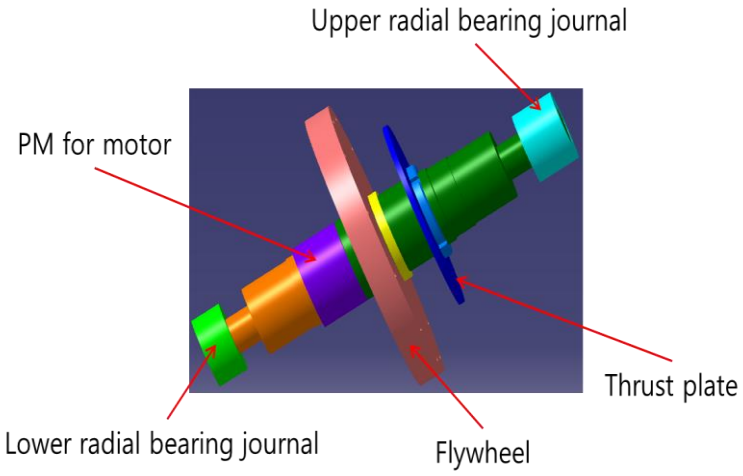

Fig. 3: Shape of the rotational rotor

The rotational rotor is composed of the upper and lower radial bearing to support the rotor in the radial direction, the thrust plate which is used for the levitation of the rotor in the horizontal direction, the flywheel to store the rotational energy, and the PM type motor to make the rotor rotate. Fig. 4 shows the FRF(Frequency Response Function) test result that has been produced from the general natural frequency test using the impact hammer. As seen in the figure the first mode is at 1,160Hz ($\cong$ 69,600rpm).

Fig. 4: FRF test result

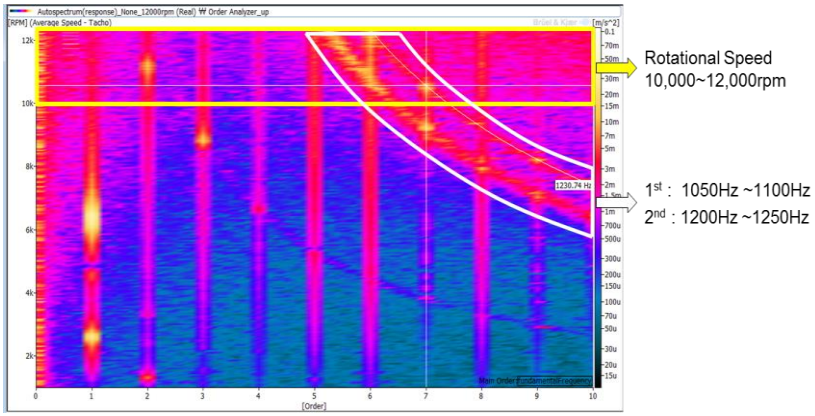

Fig. 5: Rotational modes analysis

Fig . 5 presents the measured data to analyze the relations between the rotational speed and the natural mechanical modes that appear in the rotational machine when the rotor rotates in high speed. Fig. 5 indicates that the first natural frequency appears at 1,050Hz~1,100Hz, and the rotational speed in that frequency is 10,000rpm ~ 12,000rpm that meets the 5th and 6th mechanical modes and makes the amplitude of the rotational vibration at these modes be increased. Based on these analyses the rotational speed is set to 12,000rpm to avoid the mechanical resonance in this paper. The 1st natural frequency in the FRF test is 1,160Hz and the 1st natural frequency in the rotational mode test is 1,050Hz~1,100Hz. The 60Hz frequency difference is considered as measuring error.

Manufacturing

In this section each component that consists of the flywheel energy storage system is presented.

A. Rotational rotor

Fig. 6 presents rotational rotor that has thrust plate for the rotor levitation and wheel to store the excess electrical energy. The total weight of the rotor is 23[kg].

Fig. 6: Flywheel Rotor

B. Magnetic bearings

Fig. 7 shows the radial and thrust magnetic bearings to support the rotor in radial and in axial direction. They have 500[N] and 2,500[N] maximum load capacity, respectively.

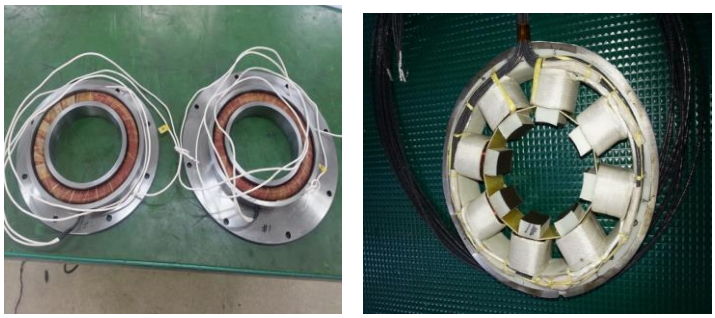

Fig. 7: Radial and axial magnetic bearings

C. Housing

Fig. 8 indicates the hosing for the flywheel energy storage system. The height and the diameter of the hosing are 585[mm] and 550[mm], respectively.

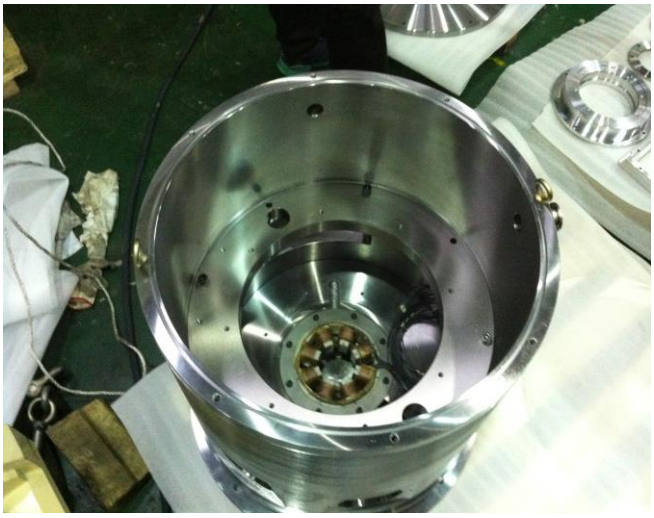

Fig. 8: Housing

Results and Discussion

A. Simulations

For the simulations of the system that mentioned in the above sections PID controllers (seen in Fig. 9) are installed to control input current of the magnetic bearings which play an important role to maintain stable air gap between magnetic bearings and the rotor. Table 1 is parameters for the simulations

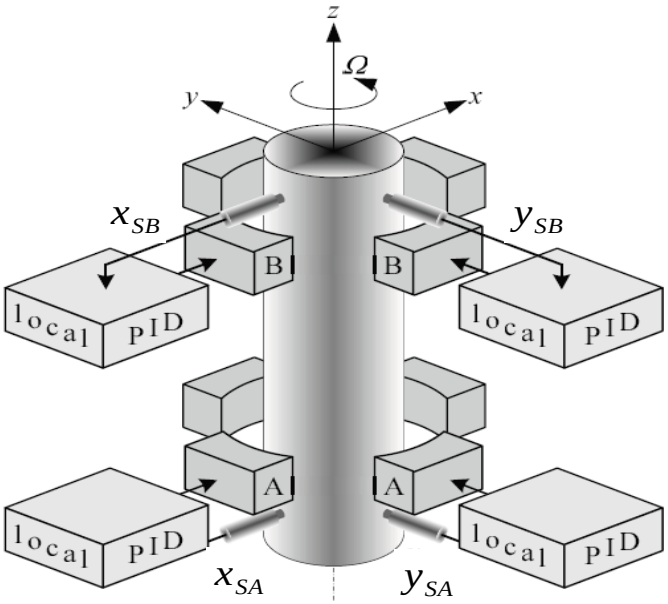

Fig. 9: Installation of PID controllers

Table 1: Parameters for the flywheel energy storage system

Variables	Value	Unit
Coil Inductance : L	50	[mH]
Coil Resistance : R	1	[Ω]
Steady Current : i_0	1	[A]
Cross Sectional Area : A	1.666×10^{-4}	[m^2]
Number of turns : N	152	[turns]
Permeability : μ_0	$4\pi\times10^{-7}$	[H/m]

Fig. 10 – 11 present simulation results. For the simulations 10[g-mm] and 100[g-mm] unbalance masses added in the rotor and the initial position of the rotor is 0.1[mm]. The red line indicates nominal airgap, 0.3[mm]. The rotational speed changes from 0[rpm] to 12,000[rpm] . As shown in the figures the trajectory of the rotor starts at the initial position (0.1[mm]) and reaches to the zero position even if there are unbalance masses (10[g-mm] and 100[g-mm]), and also the air gap deviation is very small even if the rotational speed changes from 0[rpm] to 12,000[rpm].

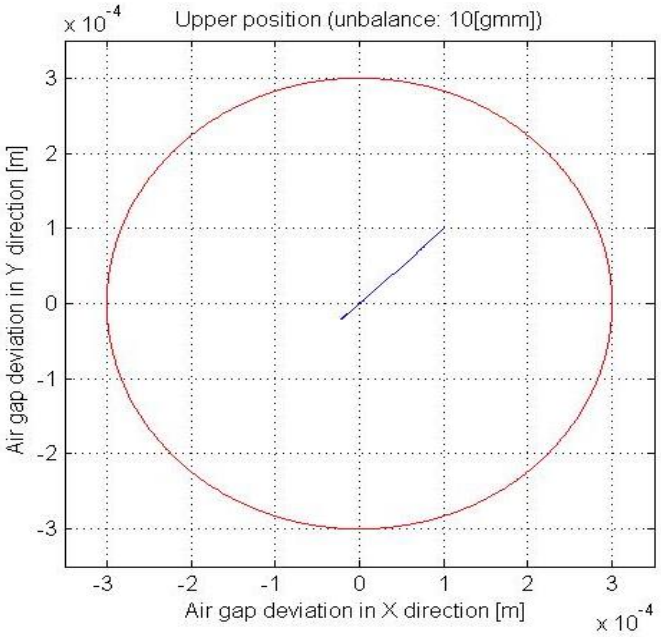

Fig. 10: Plotting in upper XY direction (10[g-mm])

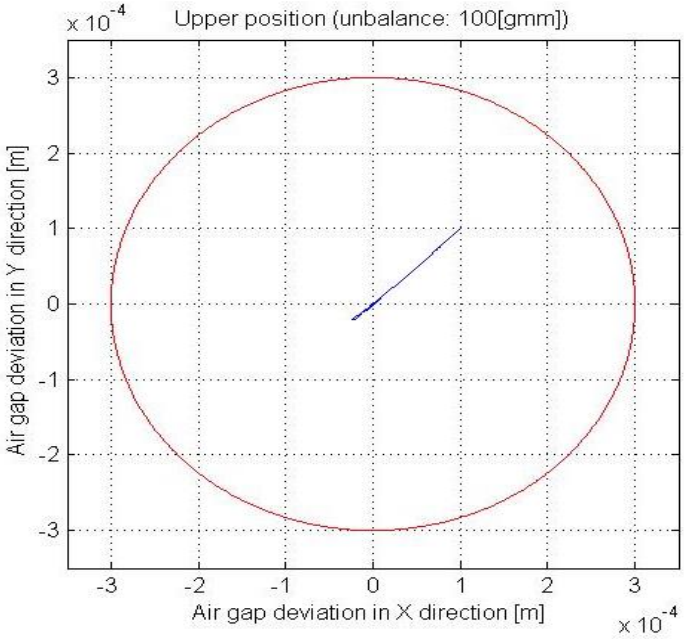

Fig. 11: Plotting in upper XY direction (100[g-mm])

B. experimental results

Fig. 12 shows the run down test results for the vacuum pump when the speed of the rotor has been increased up to the 6,000[rpm]. In the figure the blue line and the green line are for the non- vacuum and vacuum, respectively. The blue line reaches to zero speed in 178[sec] faster than that of the green line, which means the rotor rotates longer time in the vacuum.

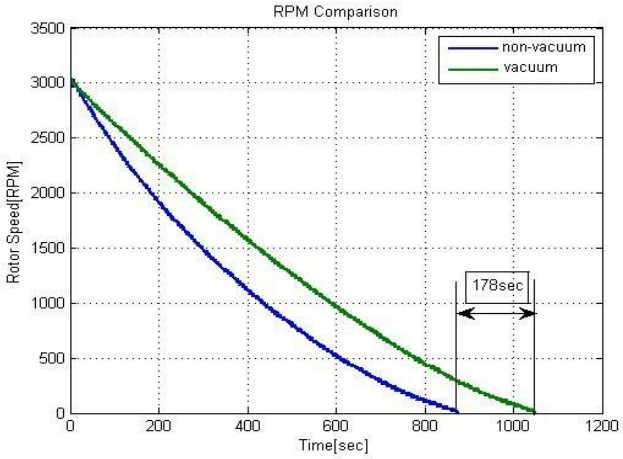

Fig. 12: Run down test for the vacuum pump

Fig 13 and 14 are the rotational test results at 12,000[rpm] that show 0.01[mm] vibration amplitude, which means that the rotational rotor is in very good center position. Natural frequency at 4,400[rpm] (rigid mode) causes the higher vibration amplitude. In these figures the red line indicates the nominal air gap distance, 0.3[mm].

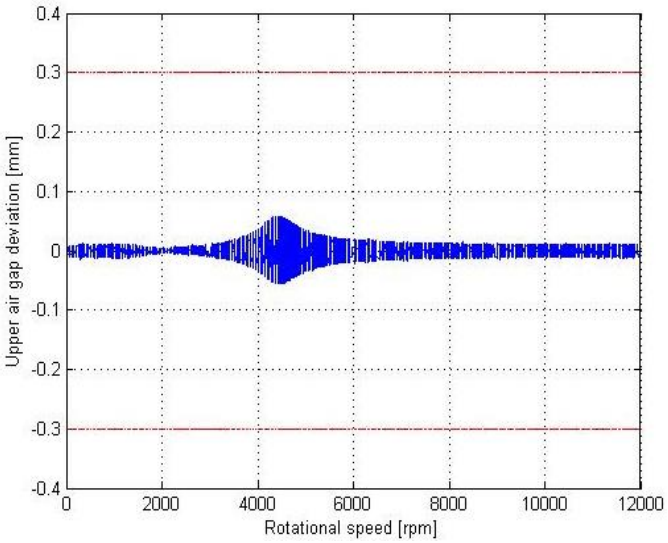

Fig. 13: Rotational speed test from 0 to 12,000rpm

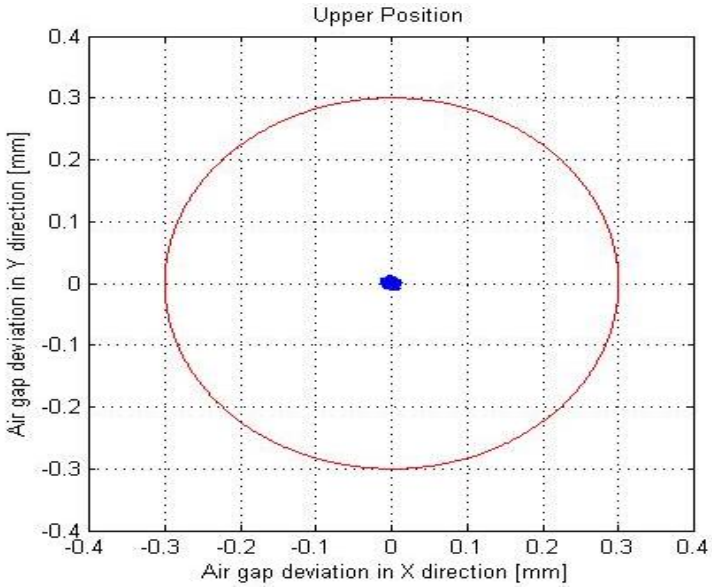

Fig. 14: Rotational speed test from 0 to 12,000rpm

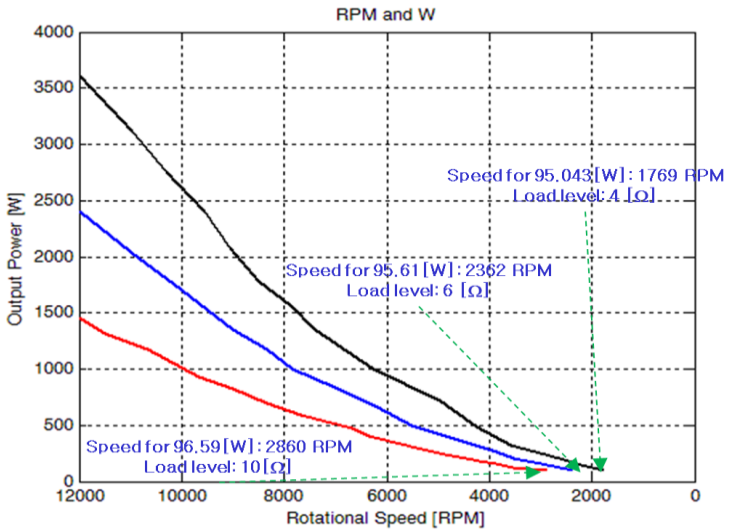

Fig. 15: Output power for the different load level

Fig. 15 presents the output power for the different load level. In case of 4[Ω] the output power at 12,000[rpm] is 3.6[kW] and it is reduced to about 96[W] at the rotational speed 1,769[rpm]. However for the lower load level (6[Ω] or 10[Ω]) than 4[Ω] the rotational speed to reach to about 96[W] is higher than that of the 4[Ω] load level, which means that higher load can use more energy.

Conclusion

In this paper the author presented flywheel energy storage system to be applied for the railway system. Mathematical model for the flywheel rotor (four-degrees-of-freedom), manufacturing of the FESS, and high speed rotational test results were shown. Output power versus different load level tests were also performed and indicated that higher load can use more energy. In the future to define the FESS efficiency various experimental tests will be performed.

References

[1] Jun-Ho Lee, *etal.* "A Study on the Design Procedure of the Eight Pole Magnetic Bearings for the Inner-rotor and the Outer-rotor type", Journal of Electrical Engineering Technology, vol. 8-6, pp. 1424-1430, 2013.

[2] J.H. Lee, A study on an effect of the flux feedback on an open-loop characteristic of the magnetic levitation system, in: 13th International Symposium on Magnetic Bearings, Washington, Virginia, USA, Aug. 6-8, 2012.

[3] J.H. Lee, P.E. Allaire, W. Jiang, T. Hu, Z. Lin, Cancellation of static and sinusoidal disturbance forces in a magnetic suspension system using exerted force and flux feedback, in: Eighth International Symposium on Magnetic Bearings, Japan, Aug. 26-28, 2002.

[4] G. Schweitzer and E. H. Maslen, eds., Magnetic Bearings: Theory, Design, and Application to Rotating Machinery, Springer, 2010.

[5] G. Schweitzer, H. Bleuler, A. Traxler, "Active Magnetic Bearings: Basics, Properties and Applications of Active Magnetic Bearings", vdf Houchschulverlag AG der ETH Zurich,1994

[6] Alan Palazzolo, *et.al*., "Aero Gravity Test of a 40,000RPM Flywheel", 13th ISMB, Arlington, Virginia, USA, August, 2012

[7] Paul, Allaire, *et.al*., "Design and analysis of the magnetic suspension system in an energy storage flywheel", 13th ISMB, Arlington, Virginia, USA, August, 2012